

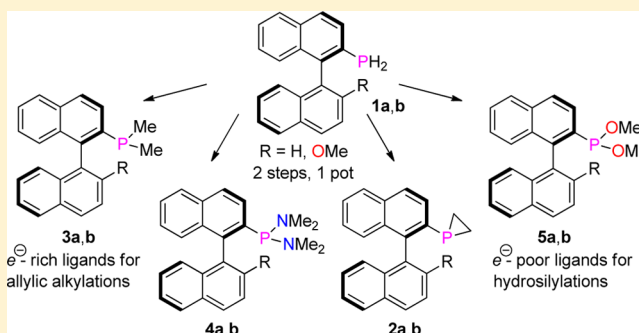
# Air-Stable Chiral Primary Phosphines: A Gateway to MOP Ligands with Previously Inaccessible Stereoelectronic Profiles

Arne Ficks, William Clegg, Ross W. Harrington, and Lee J. Higham\*

School of Chemistry, Bedson Building, Newcastle University, Newcastle upon Tyne, NE1 7RU, U.K.

## Supporting Information

**ABSTRACT:** The air-stable chiral primary phosphines **1a,b** facilitate the synthesis of previously inaccessible or hard-to-access chiral MOP-type ligands **2a,b–5a,b**, which can be prepared in one-pot reactions. These derivatives have been prepared to allow for a unique comparison of their differing structural and electronic profiles, determined here by a number of experimental and theoretical studies. Phosphiranes **2a,b** and phosphonites **5a,b** are electron-poor compounds, with the former possessing exceptional thermal stability. Conversely, the dimethylarylp phosphines **3a,b** and bis(dimethylamino)-arylp phosphines **4a,b** are good electron donors, and, in contrast to earlier reports, the dialkylarylp phosphines were found to be remarkably air-stable. The ligands were coordinated to platinum(II), and the weak *trans*-influence of the highly strained phosphiranes **2a,b** was revealed both in solution and in the solid state. The steric parameters of the ligands were investigated by the allyl rotation of their methallylpalladium(II) complexes, which showed subtle differences in exchange rates. Aryl side-on coordination of the MOP-backbone to palladium(II) was observed for complexes with a non-coordinating counterion and structurally analyzed in the case of ligand **4b**. The asymmetric induction and catalytic activity of **2a,b–5a,b** were tested in the hydrosilylation of styrene as well as the allylic alkylation of (*rac*)-(E)-1,3-diphenylallyl acetate. Major differences in reactivity were related back to the electronic parameters of the ligands.

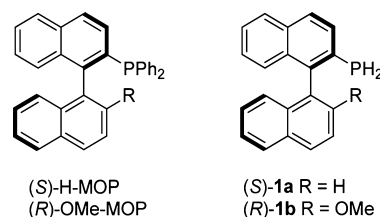


## INTRODUCTION

In transition-metal-catalyzed asymmetric synthesis, the design of the chiral ligand is crucial for transferring the stereochemical information effectively onto the substrate.<sup>1</sup> A fine balance of steric and electronic properties is often necessary to achieve high asymmetric induction while ensuring good catalytic activity. It is therefore desirable to obtain characteristic values for each ligand that describe their steric and electronic effects. The separation of electronic and steric parameters for phosphorus(III) ligands was profoundly influenced by Tolman,<sup>2</sup> and his seminal study was used as the foundation for numerous experimental and theoretical works thereafter, which have been thought-provoking for those involved in ligand design.<sup>3</sup> One impediment to the actual synthesis, comparison, and classification of related but different functionalities on a given "RP" backbone is the lack of a convenient precursor that allows for the synthesis of phosphines with electron-donating/accepting, aryl/alkyl, sterically encumbered/small, strained/open, or carbon/heteroatom functionality. Herein we show that primary phosphines **1a/b** provide such a route.

Furthermore, these precursors are the first air-stable primary phosphines that can be made in both the (*R*) and (*S*) enantiomers, in multigram quantities.<sup>4</sup> They are significant because they constitute what can be considered the parent of an important class of chiral monophosphines, Hayashi's MOP ligands (Chart 1, left),<sup>5,6</sup> which are based on an atropisomeric

Chart 1



binaphthyl skeleton and are capable of catalyzing a number of asymmetric transformations.<sup>7</sup> Importantly, because primary phosphines are readily functionalized, it ought to be possible to synthesize MOPs with stereoelectronic profiles very different from those reported to date. Prior modification of MOPs has been somewhat limited but demonstrates the significance of ligand design: different substitution in the 2'-position (most commonly H or OMe) caused major changes in the catalytic behavior,<sup>5</sup> and the aryl substituents on the phosphorus have also been modified in order to increase the catalytic performance.<sup>8</sup> Significant deviations from diaryl P-substitution (e.g., alkyl instead of aryl substituents) have seldom been introduced, as a result of synthetic difficulties in accessing these

Received: June 8, 2014

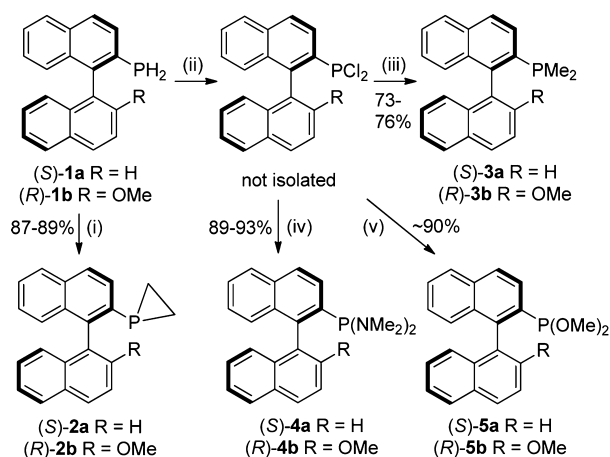
Published: November 6, 2014



derivatives via the standard methodologies used to construct these ligands.<sup>9</sup>

Primary phosphines are readily functionalized by substitution of their P-bound hydrogen atoms, but their reputation as highly air-sensitive, toxic, and pyrophoric compounds has inhibited their use in synthetic methodology.<sup>10</sup> In stark contrast to this, the chiral primary phosphines **1a,b** are both air-stable (Chart 1) by virtue of their extended  $\pi$ -conjugation, in accordance with our DFT-based model.<sup>4c</sup> Here we show that these primary phosphines facilitate the synthesis of MOP derivatives which have so far proven inaccessible or elusive, in one-pot procedures. In the first instance, we wished to compare the effect on the stereoelectronic profile of ligands that contain a highly strained phosphirane<sup>11a</sup> moiety to that of the corresponding unstrained dimethyl analogue, and therefore we prepared **2a,b** and **3a,b** (Scheme 1). Second, we wanted to

**Scheme 1. Ligand Synthesis<sup>a</sup>**



<sup>a</sup>Reaction conditions: (i) 2MeLi, Cl(CH<sub>2</sub>)<sub>2</sub>Cl, THF, -78 °C to rt; (ii) PCl<sub>5</sub>, toluene; (iii) 2MeMgCl, THF, -78 °C to rt; (iv) 2Me<sub>2</sub>NH, NEt<sub>3</sub>, THF; (v) 2MeOH, NEt<sub>3</sub>, CH<sub>2</sub>Cl<sub>2</sub>.

synthesize the novel bis(dimethylamino)phosphines **4a,b** and dimethyl phosphonites **5a,b** so as to evaluate the effect different  $\alpha$ -heteroatoms have on the ligand properties. The structural and electronic impact of the ligands is shown by a number of experimental and theoretical analyses, most notably in their palladium(II) and platinum(II) complexes, which have been studied in detail in solution and in the solid state. The ramifications of these differences in the asymmetric hydrosilylation of styrene and the asymmetric allylic alkylation of (*rac*)-(*E*)-1,3-diphenylallyl acetate will then be discussed.

## RESULTS AND DISCUSSION

**Ligand Synthesis and Stability.** The chiral phosphiranes **2a,b** possess a highly strained, three-membered phosphorus heterocycle which confers greater s-character on the donor orbital. This ultimately leads to weaker  $\sigma$ -donor, but better  $\pi$ -acceptor properties compared to their unstrained counterparts.<sup>12</sup> Despite the fact that phenylphosphirane is thermally unstable at room temperature,<sup>11</sup> **2a,b** were prepared from **1a,b** in a straightforward one-step reaction procedure to give **2a,b** in essentially quantitative yield; both ligands demonstrate exceptional thermal stability for an unconstrained phosphirane ring (Scheme 1, path (i)).<sup>11a</sup>

The dimethylphosphine analogues **3a,b** were first reported by Stryker and co-workers, but their copper hydride complexes were found to be ineffective for the reduction of ketones;<sup>9f</sup> further studies by Shi et al. were carried out on their application as catalysts in the aza-Baylis–Hillman reaction.<sup>13</sup> Synthetic pathways to obtain **3a,b** are known from earlier reports, via coupling of dimethylphosphine oxide with the appropriate binaphthyl triflate, followed by a reduction of the oxide.<sup>9f</sup> However, rather than employing a somewhat circuitous route, whereby one must first prepare the dialkylphosphine oxide, we were keen to develop an efficient one-pot synthesis, starting from our primary phosphines **1a,b**, which we have prepared efficiently on a large scale.<sup>4b</sup> After investigating a number of unsuccessful halogenation methods, we prepared the corresponding dichlorophosphines by adapting Weferling's procedure.<sup>14</sup> Thus, **1a,b** were reacted with phosphorus pentachloride in toluene to generate the respective dichlorophosphines *in situ* (Scheme 1, path (ii)), and after removal of the volatiles *in vacuo*, further reactions were performed in the same reaction vessel. Initially, we attempted the methylation by adding a solution of methyllithium in diethyl ether, but this resulted in the formation of a mixture of compounds. Instead, we found that a much cleaner reaction was achieved when methylmagnesium chloride in tetrahydrofuran was used as the methylating agent (Scheme 1, path (iii)). Analysis of the crude reaction mixtures by <sup>31</sup>P NMR showed complete conversions to the desired products (−54.0 ppm for **3a,b**), which were obtained in good yields (76%/73% respectively) after purification on silica media. The ligands were found to be air-stable after the compounds were left open to the atmosphere for 7 days, neat or in chloroform solution. This observation differs from an earlier report in which the authors stated that these compounds were air-sensitive,<sup>9f</sup> although our DFT model predicts that **3a,b** would be air-stable (SOMO energies of the radical cations are −9.05 eV (**3a**) and −8.83 eV (**3b**)).<sup>4c</sup>

While the ramifications of ring strain will be assessed by comparing the properties of **2a,b** and **3a,b**, the effect of  $\alpha$ -heteroatom substitution on the phosphorus can be established by synthesizing bis(dimethylamino)phosphines **4a,b** and the phosphonites **5a,b**. Amino substituents are known to lend  $\sigma$ -donor strength to the phosphorus, arising from electron donation of the nitrogen lone pairs.<sup>15</sup> Aminophosphines are commonly prepared by condensation reactions of phosphorus(III) halides with secondary amines.<sup>16</sup> Hence, we were able to use our primary phosphines **1a,b** as starting materials to generate the respective dichlorophosphines *in situ* (*vide supra*); these were then treated with dimethylamine under basic conditions to give **4a,b** (Scheme 1, path (iv)) in very good yields (93%/89% respectively after purification). The <sup>31</sup>P NMR spectra show typical resonances for bis-heteroatom-substituted 3-coordinated phosphines at 99.9 ppm (**4a**) and 101.0 ppm (**4b**). Ligands **4a,b** are moderately sensitive toward moisture and protic solvents such as alcohols, but purification on alumina media with reagent-grade solvents was possible, and no evidence for oxidation of these ligands in air was found. Generally, **4a,b** can be handled in air without the need for an inert environment, but they should be stored in closed vials to avoid hydrolysis on prolonged exposure to moisture.

To complete our comparative study, we synthesized the dimethyl phosphonite ligands **5a,b** from **1a,b** via methanolysis of the respective dichlorophosphine intermediates in the presence of triethylamine (Scheme 1, path (v)). The crude

products were found to decompose on silica and alumina media. The generated amine-salt impurity was therefore separated by filtration of a toluene suspension of the ligand through a pad of Celite. Ligands **5a,b** were usually obtained with >90% purity by  $^{31}\text{P}$  NMR. Their resonances in the  $^{31}\text{P}$  NMR spectra are located at lower field relative to the other ligands in this study (157.5 ppm for **5a**, 155.8 ppm for **5b**), caused by the electronegative methoxy substituents on the phosphorus atom. Ligands **5a,b** are prone to hydrolysis and should therefore be stored and handled under nitrogen.

#### Assessment of Structural and Electronic Properties.

The  $^1J_{\text{PSe}}$  coupling in  $\text{R}_3\text{P}(\text{Se})$  compounds can be used to determine the effective electronegativity of the substituents on the phosphorus atom.<sup>17</sup> The  $^1J_{\text{PSe}}$  magnitude is inversely correlated to the  $\sigma$ -donor strength of a  $\text{R}_3\text{P}$  ligand; electron-donating substituents cause the coupling constant to decrease. Sterically demanding substituents can indirectly influence the coupling if the bond angles on the phosphorus are widened; the s-character of the phosphorus lone pair is thereby reduced, resulting in increased Lewis basicity.<sup>18</sup>

The respective  $\text{ArP}(\text{Se})\text{R}_2$  derivatives were prepared by the reaction of ligands **3a,b**, **4a,b**, and **5a,b** with potassium selenocyanide.<sup>19</sup> We were unable to observe any selenide product formation for the phosphiranes **2a,b**, even at elevated temperatures and prolonged reaction times. For the  $\text{ArP}(\text{Se})\text{R}_2$  derivatives of the dimethylphosphines **3a,b** we found lower coupling constant values than for the respective derivatives of ligands **4a,b** and **5a,b**, corresponding to a better  $\sigma$ -donor character (Table 1). This is in accord with expectations, as the

**Table 1. Structural and Electronic Parameters of Phosphorus Ligands **2a,b**, **3a,b**, **4a,b**, and **5a,b****

ligand	$^1J_{\text{PSe}}^a$	$\nu(\text{CO}_{\text{Rh}})^b$	$E_{\text{HOMO}}^c$	$\text{PA}^d$	$S_4^e$
<b>2a</b>		1983	−5.72	228.0	130.1
<b>2b</b>		1985	−5.41	231.4	127.5
<b>3a</b>	685	1965	−5.59	247.3	53.5
<b>3b</b>	683	1963	−5.27	250.4	53.7
<b>4a</b>	770	1972	−5.11	254.6	52.1
<b>4b</b>	765	1969	−5.01	257.5	51.7
<b>5a</b>	858	1999	−5.69	243.0	59.5
<b>5b</b>	860	1996	−5.38	246.9	62.2

<sup>a</sup>Coupling from the  $\text{ArP}(\text{Se})\text{R}_2$  derivative in Hz. <sup>b</sup> $\text{CO}$  stretch of  $\text{trans}[\text{RhCl}(\text{CO})(\text{ArPR}_2)_2]$  in  $\text{CH}_2\text{Cl}_2$  in  $\text{cm}^{-1}$ . <sup>c</sup>Calculated HOMO energies in eV of the optimized structures of the free ligand. <sup>d</sup>Calculated proton affinity in kcal/mol. <sup>e</sup>Calculated from the optimized structure of the free ligand in degrees. See text for further definition of the  $S_4$  parameter.

electronegative nitrogen atoms in **4a,b** and, to a greater extent, the oxygen atoms in **5a,b** reduce the  $\sigma$ -donor strength of the phosphorus atom.

In order to include phosphiranes **2a,b** in a comparative study of electronic properties, we synthesized  $\text{trans}[\text{Rh}(\text{L}_p)_2(\text{CO})\text{Cl}]$  complexes ( $\text{L}_p$  = phosphorus ligand) and measured the symmetric carbonyl stretching frequencies in their IR spectra. A higher vibrational wavenumber indicates a lower net-donor property of  $\text{L}_p$ , as the reduced electron density on the metal allows for less back-bonding into the antibonding  $\pi^*$ -orbitals of the carbonyls.<sup>20</sup> The IR spectra were recorded in dichloromethane solution, since packing effects in the solid state may have a significant influence on the observed values.<sup>21</sup> We found that **3a,b** are the strongest net donors (1965, 1963  $\text{cm}^{-1}$ ),

followed by **4a,b** (1972, 1969  $\text{cm}^{-1}$ ), **2a,b** (1983, 1985  $\text{cm}^{-1}$ ), and **5a,b** (1999, 1996  $\text{cm}^{-1}$ ). The weak donating properties of phosphiranes **2a,b** compared to their dimethylphosphine counterparts **3a,b** can be attributed to their pyramidalized structures, which result in increased s-character of the donor orbitals. As such, phosphiranes **2a,b** show weaker net donation than  $\text{PPh}_3$  (1979  $\text{cm}^{-1}$ ) but are better donors than the  $^i\text{PrBABAR-Phos}^{22}$  phosphirane ligand (1991  $\text{cm}^{-1}$ ), in which the three-membered ring is encapsulated into a rigid backbone.<sup>20a,22a</sup>

Electronic descriptors measuring the donor abilities of our ligands were calculated from their HOMO orbital energy levels and proton affinity (PA) in a series of DFT calculations (calculated at the B3LYP/6-31G\* level of theory). For tertiary phosphines, the energy of the HOMO typically corresponds to the lone pair of the phosphorus, and PA is a measure of its  $\sigma$ -basicity; the two values have been found to correlate fairly well for a range of phosphorus ligands.<sup>23</sup> The HOMO energies were calculated from the optimized structures of the free ligands and are given in Table 1. We observed lower  $E_{\text{HOMO}}$  values in the direct comparison of H-MOP derivatives (**a** ligand series) to their respective OMe-MOP counterparts (**b** ligand series). The spatial representations of the HOMO orbitals (Figure 1) reveal

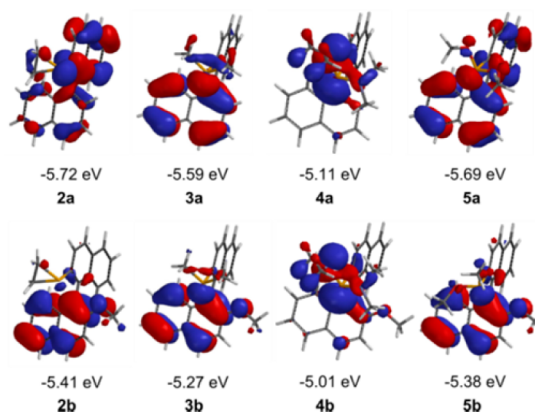


**Figure 1.** HOMO energies of **2a,b**–**5a,b** calculated at the B3LYP/6-31G\* level of theory.

their distribution on the binaphthyl backbone and also on the methoxy group in the OMe-MOP derivatives (**b**). It is interesting how the 2' substituent significantly affects the calculated HOMO energies: The presence of the methoxy group causes a general increase in the HOMO energy for the "**b**" series of ligands, which implies improved  $\sigma$ -donor properties relative to its analogue in the "**a**" series. Inspection of the HOMO energies in Table 1 shows, somewhat surprisingly, that the dimethyl-substituted phosphine **3a** has a calculated HOMO energy sandwiched between those of the phosphiranes **2a** and **2b**.

In contrast to this, the PA values allow for ranking according to ligand type, rather than backbone substitution (Table 1). The energy was calculated from the differential in molecular energies of the DFT-optimized structure of the free ligand and the optimized structure of the protonated ligand (protonated on the phosphorus).<sup>23,24</sup> Their magnitude increases (indicating an increasing  $\sigma$ -basicity) in the order **2a,b** < **5a,b** < **3a,b** < **4a,b**. In comparison to the relative trend of the net donor properties from the experimentally determined values for  $\nu(\text{CO}_{\text{Rh}})$ , it appears that the calculated  $\sigma$ -basicity suggested by both the



HOMO and PA values may be somewhat overestimated for the heteroatom-substituted derivatives. This is further evidence that caution ought to be used when rationalizing experimental behavior from the calculation of relatively simple parameters in isolation.

To gain insight into the structural properties of the ligands, we next calculated the symmetric deformation coordinate. The  $S_4'$  parameter, introduced by Orpen et al.,<sup>25</sup> is an alternative to Tolman's cone angle ( $\theta_T$ ).<sup>2,26</sup> Its use is appropriate for MOP-type compounds in particular, since the  $\theta_T$  parameter would be dominated by the bulky binaphthyl group.<sup>27</sup> As a measure of flattening or pyramidalization around the phosphorus,  $S_4'$  is defined as the sum of Z–P–R angles ( $\alpha_i$ ) minus the sum of R–P–R angles ( $\beta_i$ ), with Z describing the coordinated atom of the ligand (Figure 2). A modified descriptor,  $S_4$ , is used for free

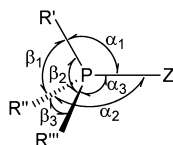


**Figure 2.** Calculation of  $S_4' = (\alpha_1 + \alpha_2 + \alpha_3) - (\beta_1 + \beta_2 + \beta_3)$ .

ligands, where Z is a vector perpendicular to the plane containing the three substituents of the phosphorus.<sup>28</sup> The  $S_4$  values were determined from the optimized minimal energy geometries of each ligand at the B3LYP/6-31G\* level (Table 1). The pyramidalization of the phosphiranes **2a,b** is recognized by unusually large  $S_4$  values (130.1° and 127.5°, respectively). In contrast, **3a,b** and **4a,b** exhibit much smaller  $S_4$  values of similar magnitudes (51.7°–53.7°), which is unsurprising in the absence of ring strain. The values are increased for **5a,b** (59.5° and 62.2°, respectively) in comparison to the other unstrained derivatives.

**Platinum(II) Coordination Properties.** To investigate the structural and electronic behavior of our ligands upon coordination to a metal center, we prepared a series of square planar platinum(II) complexes. Solution studies of these compounds can give an insight into the nature of the phosphorus–platinum bonds by virtue of the  $^1J_{\text{PPt}}$  coupling constants in their NMR spectra.<sup>29</sup> It has been suggested that the main contributor to the one-bond coupling is the Fermi interaction of the two nuclei involved.<sup>30</sup> This means that the s-component of the P–Pt bond has a direct influence on the coupling constant, yielding larger values with increasing s-orbital overlap. However, p- and d-effects will indirectly affect the s-orbital interaction; previous reports have shown that there is a good correlation between the  $^1J_{\text{PPt}}$  magnitude and the Pt–P bond length.<sup>31</sup> This relationship allows for the determination of *cis* and *trans* influences in platinum complexes, i.e., the ability of a ligand to weaken the bond to a substituent in the *cis/trans* position,<sup>32</sup> which then helps in rationalizing the  $\sigma$ -donor and  $\pi$ -acceptor properties of the ligands.<sup>33,34</sup> Complementary studies, using X-ray crystallographic analysis to determine the bond lengths, are available to supplement the data acquired in solution.

Platinum(II) dichloride complexes with the general formula  $[\text{Pt}(\text{L}_\text{P})_2\text{Cl}_2]$  ( $\text{L}_\text{P}$  = phosphorus ligand) were synthesized from the reaction of *cis*- $[\text{Pt}(\eta^4\text{-cod})\text{Cl}_2]$  with the appropriate ligand (Figure 3). In solution and in the solid state, the selective formation of *cis*-**6a,b** or *cis*-**7b** (Figure 4) was observed when phosphiranes **2a,b** or dimethylphosphine **3b**, respectively, were

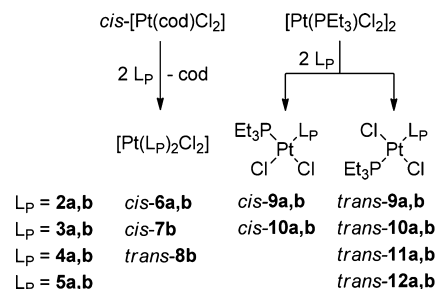


**Figure 3.** Numbering of the platinum complexes used in this study ( $\text{L}_\text{P}$  = phosphorus ligand).

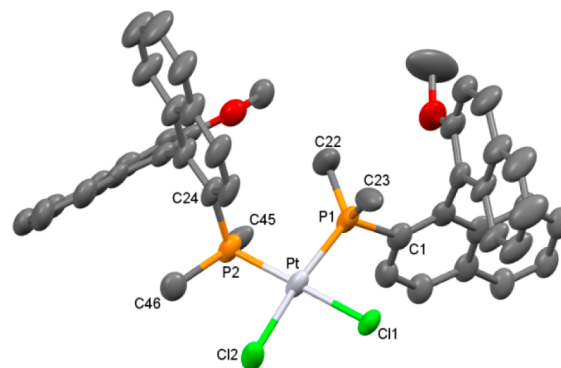


**Figure 4.** Molecular structure of *cis*- $[\text{Pt}(\mathbf{3b})_2\text{Cl}_2]$  (*cis*-**7b**) with 50% probability displacement ellipsoids. Hydrogen atoms and solvent molecules omitted for clarity.

used as ligands. Under the same reaction conditions **4b** gave *trans*-**8b** (Figure 5) with complete selectivity. The  $^{31}\text{P}$  NMR

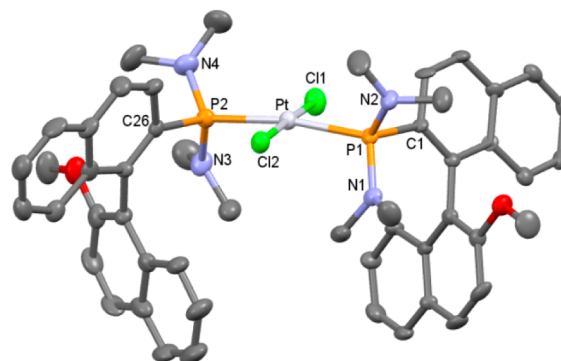


**Figure 5.** Molecular structure of *trans*- $[\text{Pt}(\mathbf{4b})_2\text{Cl}_2]$  (*trans*-**8b**) with 50% probability displacement ellipsoids. Hydrogen atoms are omitted for clarity.

spectra show the expected singlet resonance together with satellites for the doublet produced by coupling to  $^{195}\text{Pt}$ ; for the *cis* complexes the  $^1J_{\text{PPt}}$  coupling is larger in *cis*-**6a,b** (4170, 4160 Hz) compared to *cis*-**7b** (3647 Hz) as a result of the higher s-character of the phosphirane donor orbitals.<sup>11</sup> The  $^1J_{\text{PPt}}$  coupling in *trans*-**8b** (2955 Hz) is significantly smaller compared to the *cis* complexes, because of the stronger reciprocal *trans* influence of the phosphine ligands compared to the *trans* influence of a chloride ligand. Selected bond lengths and angles for the solid-state structures of *cis*-**6a,b**, *cis*-**7b**, and *trans*-**8b** are given in Table 2.

Phosphirane complexes *cis*-**6a,b** form shorter Pt–P bonds (2.204(3)–2.212(2) Å) than the dimethylphosphine derivative

Table 2. Selected Bond Distances (Å), Angles (°), and  $S_4'$  Data from X-ray Crystallographic Analysis

	<i>cis</i> -6a <sup>11</sup>	<i>cis</i> -6b <sup>11,a</sup>	<i>cis</i> -7b	<i>trans</i> -8b	<i>trans</i> -9b	<i>trans</i> -11a
Pt–P1	2.212(2)	2.204(3)	2.241(4)	2.307(3)	2.304(3)	2.3395(15)
Pt–P2	2.209(2)		2.241(3)	2.313(3)	2.284(3)	2.3050(15)
Pt–Cl1	2.337(2)	2.338(3)	2.368(3)	2.292(3)	2.293(3)	2.3001(13)
Pt–Cl2	2.334(2)		2.339(3)	2.302(3)	2.307(2)	2.3080(14)
P1–Pt–P2	97.02(8)	96.92(14)	96.53(13)	170.37(10)	178.76(12)	176.90(5)
P1–Pt–Cl1	175.90(10)	169.05(10)	83.40(12)	92.05(10)	90.86(9)	92.34(5)
P1–Pt–Cl2	85.40(9)		172.69(12)	87.93(9)	88.32(9)	91.41(5)
P2–Pt–Cl1	87.06(10)	87.28(7)	178.45(13)	87.74(10)	88.05(10)	85.15(5)
P2–Pt–Cl2	177.57(10)		90.73(13)	91.87(10)	92.77(9)	91.25(5)
Cl1–Pt–Cl2	90.52(8)	90.42(15)	89.36(11)	177.54(11)	178.25(15)	173.86(6)
$S_4'$ (P1)	98.0	105.4	24.3	21.3	105.7	18.7
$S_4'$ (P2)	103.6		17.9	21.5	24.0	27.8

<sup>a</sup>Two-fold rotational symmetry.

*cis*-7b (2.241(4) Å, 2.241(3) Å), which is attributed to their more pyramidalized structure.

The Pt–P bond lengths are further elongated in *trans*-8b (2.307(3) Å, 2.313(3) Å) due to the relatively strong reciprocal *trans* influence, in agreement with the NMR data. The strong pyramidalization of the phosphirane group is retained upon complexation and manifests itself in large  $S_4'$  values for *cis*-6a,b (98.0–105.4°; calculated from X-ray data). For *cis*-7b and *trans*-8b the adjacent groups around the phosphorus are only slightly tilted out of the plane, resulting in much smaller  $S_4'$  values (17.9–21.5°).

For further evaluation of the relative *cis* and *trans* influences, we synthesized unsymmetrical platinum(II) complexes with the formula [Pt(P<sub>L</sub>)(PEt<sub>3</sub>)Cl<sub>2</sub>] (selected NMR data are given in Table 3).<sup>24</sup> The reaction of two equivalents of phosphorus ligand (P<sub>L</sub>) with [Pt(PEt<sub>3</sub>)Cl<sub>2</sub>]<sub>2</sub> proceeded quantitatively in all instances (Figure 3). In the case of phosphiranes 2a,b and dimethylphosphines 3a,b, we observed the formation of both *cis* and *trans* isomers of the corresponding platinum complexes

Table 3. Selected NMR Spectroscopic Data of the Platinum Complexes Prepared in This Study

complex	$\delta(\text{Pt})^a$	$\delta(\text{P}_1)^b$	$^1J_{\text{PtP}(\text{P}_1)}^c$	$\delta(\text{P}_2)^d$	$^1J_{\text{PtP}(\text{P}_2)}^e$
<i>cis</i> -6a	n.d. <sup>f</sup>	−149.2	4170		
<i>cis</i> -6b	n.d. <sup>f</sup>	−149.3	4160		
<i>cis</i> -7b	−4362	−6.1	3647		
<i>cis</i> -9a	−4493	−144.1	4381	10.4	3281
<i>cis</i> -9b	−4501	−144.1	4377	9.8	3282
<i>cis</i> -10a	−4401	−5.1	3725	7.1	3412
<i>cis</i> -10b	−4412	−2.9	3737	7.2	3404
<i>trans</i> -8b	−3747	87.8	2955		
<i>trans</i> -9a	−3941	−149.6	2570	15.5	2871
<i>trans</i> -9b	−3921	−151.9	2566	13.8	2886
<i>trans</i> -10a	−3914	−4.5	2364	12.5	2479
<i>trans</i> -10b	−3917	−1.3	2402	12.0	2464
<i>trans</i> -11a	−3869	90.4	3030	10.7	2365
<i>trans</i> -11b	−3839	90.4	3049	10.4	2332
<i>trans</i> -12a	−3881	119.8	3428	10.4	2402
<i>trans</i> -12b	−3859	117.3	3454	8.9	2407

<sup>a</sup>Chemical shift in ppm. <sup>b</sup>Resonance of the ArPR<sub>2</sub> ligand in ppm. <sup>c</sup>Coupling of the ArPR<sub>2</sub> ligand in Hz. <sup>d</sup>Resonance of the PEt<sub>3</sub> ligand in ppm. <sup>e</sup>Coupling of the PEt<sub>3</sub> ligand in Hz. <sup>f</sup>Not determined due to solubility issues.

9a,b and 10a,b in solution. The two respective isomers can be distinguished by their  $^2J_{\text{PP}}$  coupling constants in the  $^{31}\text{P}$  NMR spectra. The *trans* complexes show a characteristic large  $^2J_{\text{PP}}$  coupling (482–575 Hz) while the equivalent coupling for the corresponding *cis* isomers is much smaller (18–24 Hz, Figure 6). The ratios of *cis* and *trans* isomers varied from 2:1 to 1:2

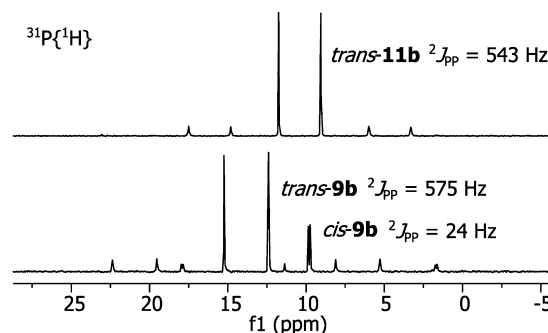
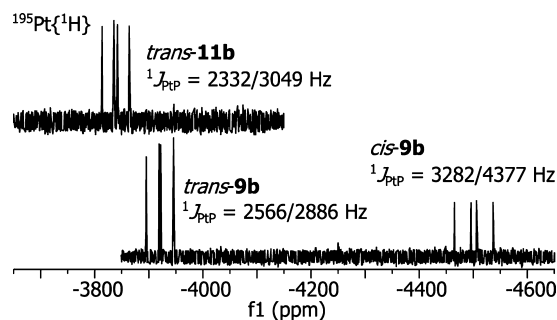


Figure 6.  $^{31}\text{P}\{^1\text{H}\}$  NMR spectra of [Pt(2b)(PEt<sub>3</sub>)Cl<sub>2</sub>] (*cis*-9b and *trans*-9b isomers present) and [Pt(4b)(PEt<sub>3</sub>)Cl<sub>2</sub>] (only *trans*-11b isomer present).

depending on the ligand. NOESY experiments showed no exchange of the two isomers on the NMR time scale, and additional NMR spectra that were recorded after leaving the complexes in solution for 24 h yielded unchanged *cis*/*trans* ratios. In previous reports about related platinum(II) complexes the *trans* products have been found to convert to their *cis* isomers over time.<sup>35</sup> When the bis(dimethylamino)phosphines 4a,b or the dimethyl phosphonites 5a,b were used as ligands, the *trans*-11a,b or *trans*-12a,b isomers were formed exclusively, displaying typical  $^2J_{\text{PP}}$  coupling constants of 543–604 Hz in their  $^{31}\text{P}$  NMR spectra (Figure 6 shows 11b).

The fast relaxation time of the platinum nucleus in the compounds enabled the collection of  $^{195}\text{Pt}$  NMR spectra (Figure 7). For the [Pt(P<sub>L</sub>)(PEt<sub>3</sub>)Cl<sub>2</sub>] series, resonances for the *trans* complexes are observed downfield (−3839 to −3941 ppm) to the corresponding *cis* isomers (−4401 to −4501 ppm, Table 3). The phosphiranes in *cis*-9a,b induce strong shielding of the platinum nucleus and show an upfield shift of ~100 ppm compared to *cis*-10a,b. The strongest deshielding effects were found for complexes of the heteroatom-substituted ligands in *trans*-11a,b and *trans*-12a,b (−3839 to −3881 ppm).



**Figure 7.**  $^{195}\text{Pt}\{^1\text{H}\}$  NMR (108 MHz) spectra of **9b** (*cis* and *trans* isomers present) and *trans*-**11b**.

The magnitude of  $^1J_{\text{PtP}}$  for the  $\text{PEt}_3$  ligand in  $[\text{Pt}(\text{P}_\text{L})(\text{PEt}_3)\text{Cl}_2]$  corresponds well to the Pt– $\text{PEt}_3$  bond length (*vide supra*) and can therefore be used as a probe to determine the relative *cis/trans* influences of various phosphorus ligands ( $\text{P}_\text{L}$ ). A smaller coupling is indicative of a larger *cis/trans* influence of the potential ligand. The *trans* influence for the phosphirane ligands in *trans*-**9a,b** is comparatively weak in relation to the dimethylphosphine ligands in *trans*-**10a,b** (2871/2886 Hz versus 2479/2464 Hz). The situation is reversed for the *cis* influence which is stronger for the phosphiranes in *cis*-**9a,b** compared to *cis*-**10a,b** (3281/3282 Hz versus 3412/3404 Hz). The *trans* influence observed in *trans*-**12a,b** (2402/2407 Hz) and *trans*-**11a,b** (2365/2332 Hz) is subsequently further strengthened; data accounting for the *cis* influence in these compounds are unavailable due to the selective formation of the *trans* isomers only.

The rationale for the unusually strong *cis* influence in **9a,b** lies in the higher s-character of the phosphirane donor orbital, caused by its more strongly pyramidalized structure (Figure 8).

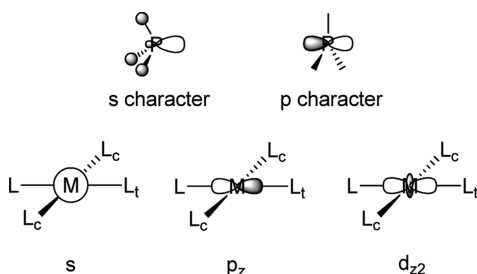


**Figure 8.** Models of P-ligand and metal-centered orbitals. Ligands with higher s-character donor orbitals interact with metal-centered s orbitals, weakening *cis* and *trans* substituents, whereas those with more p-character interact with p and d orbitals on the metal and show predominantly *trans* influence.

The interaction of the donor orbital with a symmetric metal-centered s-orbital results in weakened bonds to both *cis* and *trans* ligands in **9a,b**. In contrast, the *trans* influence is stronger in **10a,b** with a smaller *cis* influence, because the increased p-character of the ligand donor orbital mainly weakens the bond to the ligand in the *trans* position, while there is only a small overlap to the orbitals of the ligands in the *cis* position. The further increased *trans* effect in **11a,b** and **12a,b** is an indication of the predominantly p-character of the respective phosphorus donor orbitals in **4a,b** and **5a,b**.

Slow evaporation from dichloromethane solutions of *trans*-**9b** (Figure 9) and *trans*-**11a** (Figure 10) yielded crystals suitable for X-ray analysis (selected structural parameters are given in

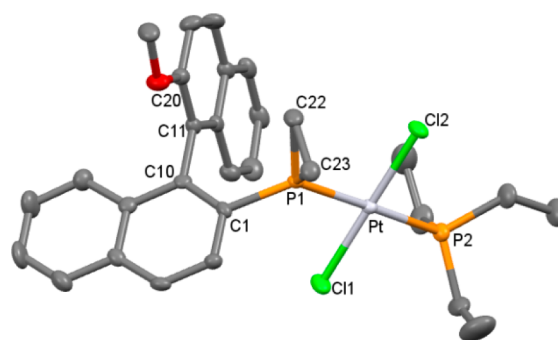


**Figure 9.** Molecular structure of *trans*- $[\text{Pt}(\text{2b})(\text{PEt}_3)\text{Cl}_2]$  (*trans*-**9b**) with 50% probability displacement ellipsoids. Hydrogen atoms omitted for clarity.

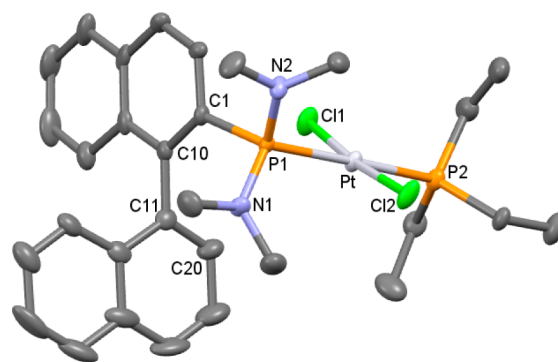


**Figure 10.** Molecular structure of *trans*- $[\text{Pt}(\text{4a})(\text{PEt}_3)\text{Cl}_2]$  (*trans*-**11a**) with 50% probability displacement ellipsoids. Hydrogen atoms omitted for clarity.

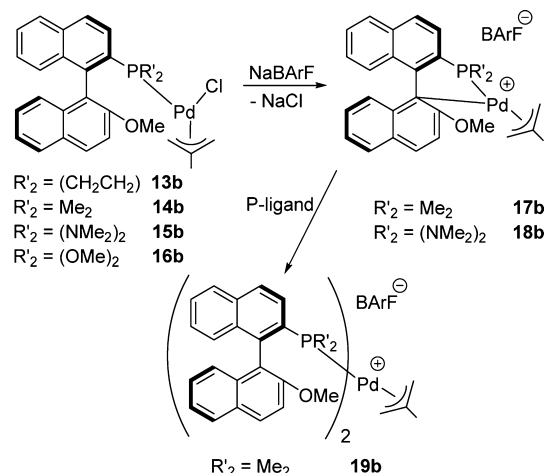
Table 2). The large  $S_4'$  value of the phosphirane ligand in *trans*-**9b** ( $105.7^\circ$ ) indicates the strain caused by the heterocycle; the  $S_4'$  value of the unstrained bis(dimethylamino)phosphine ligand in *trans*-**11a** is only  $18.7^\circ$ . The Pt–P bond length of the  $\text{PEt}_3$  ligand is shorter in *trans*-**9b** ( $2.284(3)$  Å) compared to *trans*-**11a** ( $2.3050(15)$  Å), which is in agreement with the solution NMR data and confirms the weak *trans* influence of the phosphirane ligand.

The phosphirane–platinum bond length in *trans*-**9b** is shorter compared to that in the bis(dimethylamino)phosphine complex *trans*-**11a** ( $2.304(3)$  versus  $2.3395(15)$  Å), a result of the more pyramidalized structure of the phosphirane.

**Palladium(II) Coordination.** We next studied the coordination chemistry of **2b–5b** on palladium(II), which is often the metal of choice for catalytic reactions of MOP-type ligands;<sup>5b</sup> the reaction of chloro(2-methylallyl)palladium dimer with the appropriate phosphine gave the respective palladium chloride complexes **13b–16b** (Scheme 2). For all these complexes, the formation of two different isomers was evident by the appearance of two independent resonances in the  $^{31}\text{P}$  NMR spectra, as a consequence of the selective orientation of the methylallyl group. In the NOESY spectra, we identified a rapid exchange process caused by the selective  $\eta^3\text{--}\eta^1\text{--}\eta^3$  interchange mechanism of the methylallyl fragment that resulted in broadened peaks at room temperature. During that process the protons in the *cis* position exchange in a *syn/anti* fashion, while a *syn/syn* and *anti/anti* exchange is observed for the protons in the *trans* position.<sup>36</sup> The selective opening of the allyl ligand in the *trans* position is due to the stronger *trans* effect of the P-donor ligand compared to the chloride ligand.



Scheme 2. Pd(II) Complexes of 2b, 3b, 4b, and 5b



Cooling to  $-25\text{ }^\circ\text{C}$  gave rise to sharpened resonances, which allowed for the assignment of the two isomers appearing in  $\sim 2:1$  (**13b**, **14b**),  $\sim 3:2$  (**15b**), and  $\sim 9:1$  (**16b**) ratios. Quantitative analysis of the peak integrals in the NOESY spectra at  $-25\text{ }^\circ\text{C}$  yielded exchange rate constants of  $k_{\text{AB}} \approx 0.8\text{ s}^{-1}$  and  $k_{\text{BA}} \approx 1.3\text{ s}^{-1}$  for **13b**,  $k_{\text{AB}} \approx 0.4\text{ s}^{-1}$  and  $k_{\text{BA}} \approx 0.7\text{ s}^{-1}$  for **14b**,  $k_{\text{AB}} \approx 0.1\text{ s}^{-1}$  and  $k_{\text{BA}} \approx 0.2\text{ s}^{-1}$  for **15b**, and  $k_{\text{AB}} \approx 0.3\text{ s}^{-1}$  and  $k_{\text{BA}} \approx 3.1\text{ s}^{-1}$  for **16b**. The same experiment at  $-50\text{ }^\circ\text{C}$  showed no evidence of exchange.

In the case of **14b**, slow diffusion of diethyl ether into a dichloromethane solution yielded crystals suitable for X-ray crystallographic analysis (Figure 11).

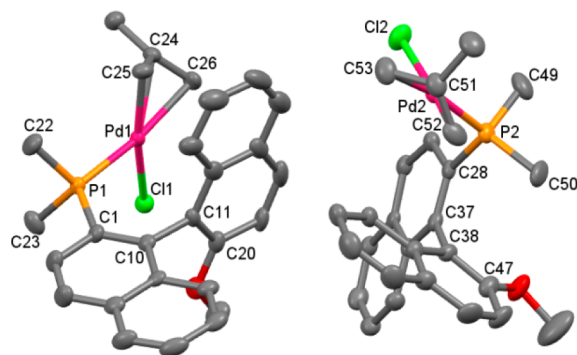


**Figure 11.** Molecular structure of  $[\text{Pd}(\mathbf{3b})(\eta^3\text{-C}_4\text{H}_7)\text{Cl}]$  (**14b**) with 50% probability displacement ellipsoids. Hydrogen atoms and solvent molecule omitted for clarity. Selected bond distances (Å) and angles ( $^\circ$ ): Pd1–P1 2.2967(11), Pd1–Cl1 2.3721(12), Pd1–C24 2.187(4), Pd1–C25 2.108(4), Pd1–C26 2.200(4), Pd2–P2 2.2686(13), Pd2–Cl2 2.3554(13), Pd2–C51 2.154(5), Pd2–C52 2.095(5), Pd2–C53 2.204(5); P1–Pd1–Cl1 93.78(4), P1–Pd1–C25 99.98(16), Cl1–Pd1–C25 166.18(15), P2–Pd2–Cl2 91.25(5), P2–Pd2–C52 101.04(17), Cl2–Pd2–C52 167.70(17), C1–C10–C11–C20  $-91.2(6)$ , C28–C37–C38–C47  $-101.0(4)$ .

The structure contains two independent isomers which have the (2-methylallyl)palladium unit in different orientations. Pd–P bond lengths are 2.2967(11) and 2.2686(13) Å, shorter than for the two MOP-phosphine allylpalladium complexes previously reported (2.3098(9) and 2.3279(9) Å).<sup>37</sup> MOP ligands are able to utilize their aromatic backbone to coordinate to a vacant metal site in a chelating P,C- $\sigma$ -donor or P,C- $\pi$ -arene bidentate fashion.<sup>38,39</sup> The reaction of **14b** and **15b** with

NaBARF was carried out to exchange the chloride for a non-coordinating BARF-anion, giving complexes **17b** and **18b** (Scheme 2). This frees up a binding site and allows for coordination of the naphthyl group. We were able to obtain the crystal structure of the bis(dimethylamine) derivative **18b** which clearly illustrates the P,C coordination mode in the solid state. The distance between the palladium atom and the bonded carbon C11 on the naphthyl ring is 2.302(4) Å (Figure 12). The position of the palladium above the naphthyl ring is

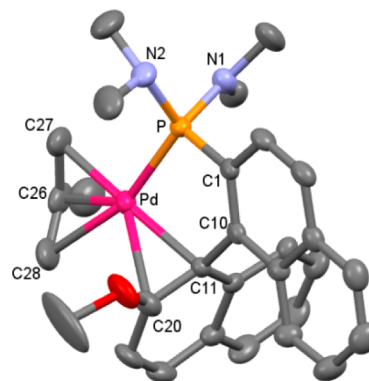


**Figure 12.** View of the molecular structure of  $[\text{Pd}(\mathbf{4b})(\eta^3\text{-C}_4\text{H}_7)]\text{BARF}$  (**18b**) with 50% probability displacement ellipsoids. Hydrogen atoms, the BARF anion, and solvent molecule have been omitted for clarity. Selected bond distances (Å) and angles ( $^\circ$ ): Pd–P 2.2553(11), Pd–C11 2.302(4), Pd–C20 2.554, Pd–C26 2.194(5), Pd–C27 2.110(5), Pd–C28 2.232(5), N1–P 1.653(4), N2–P 1.683(4), C11–C20 1.400(6), C26–C27 1.435(7), C26–C28 1.373(8); P–Pd–C11 82.21(10), P–Pd–C20 104.05(11), P–Pd–C27 97.26(14), C11–Pd–C28 114.16(18), C20–Pd–C28 88.06(19), C1–C10–C11–C20  $-101.7(5)$ .

moved slightly toward C20, to which the distance is 2.554 Å. The Pd–P distance was found to be 2.2553(11) Å and relates well to other MOP-type complexes as described above. Interestingly, the two P–N bond lengths and angles are inequivalent and show a peculiar pattern. The phosphorus atom carries a shorter bonded planar N atom (N1–P distance 1.653(4) Å, sum of angles around N1  $357.7^\circ$ ) and a longer bonded N atom that shows a more pyramidal geometry (N2–P distance 1.683(4) Å, sum of angles at N2  $342.7^\circ$ ). The pattern is much less pronounced in the platinum structures *trans*-**8b** (Figure 5) and *trans*-**11a** (Figure 10), which show only minor distortions around the N atom (sum of angles  $355.9\text{--}360.0^\circ$ ). It is assumed that the planarity of the nitrogen arises from electron donation of its lone pair toward the phosphorus.<sup>15</sup>

In solution, we observed the formation of two isomers in a 1:1 ratio for both **17b** and **18b** (caused by rotation of the methylallyl group). As the coordination sphere of the palladium atom is filled by side-on bonding to the C1'-carbon (labeled as C11 in the X-ray structure of **18b**), we consequently found an upfield shift of C1' by about 20 ppm in the  $^{13}\text{C}$  NMR spectra compared to the free ligands **3b** and **4b** and the palladium chloride complexes **14b** and **15b**. The NOESY spectrum of **17b** showed exchange of the two isomers at room temperature. Interestingly, we detected *syn/anti* exchange<sup>36</sup> as well as an apparent allyl rotation,<sup>40</sup> in a relative ratio of 2:3. Quantitative analysis of the methoxy resonances in the NOESY spectrum yielded a combined total exchange rate of  $k_{\text{AB}} \approx k_{\text{BA}} \approx 0.2\text{ s}^{-1}$ . The exchange rate is therefore smaller than for the related allylpalladium chloride complexes **14b**, which gave exchange

rates of that magnitude at much lower temperature ( $-25\text{ }^{\circ}\text{C}$ , *vide supra*). The NOESY spectrum of **18b** showed no exchange at room temperature.

We were also interested in coordinating two phosphorus ligands to the palladium center, since these species may form as intermediates in catalytic reaction cycles.<sup>41,42</sup> The addition of one equivalent of dimethylphosphine ligand **3b** to complex **17b** resulted in the quantitative formation of **19b** (Scheme 2). The product was analyzed by NMR and HRMS; unfortunately, we were unable to obtain crystals for X-ray diffraction. The  $^{13}\text{C}$  NMR spectrum gave no further evidence of aryl coordination. The vacated coordination site from the dissociated C1'-carbon of **17b** was filled by the added phosphorus donor. One single isomer was observed in the  $^{31}\text{P}$  NMR spectrum in the form of two doublet resonances at  $-2.1$  and  $-7.6$  ppm with a mutual coupling of  $^2J_{\text{PP}} = 43$  Hz. We suspect that the induced symmetry by coordination of two equivalent phosphorus ligands leads to identical structures upon allyl rotation. We detected no dynamic behavior in the NOESY NMR at room temperature, presumably because of the crowded coordination sphere around the metal. We were unable to isolate equivalent products using ligands **2b**, **4b**, or **5b**.

**Asymmetric Hydrosilylation.** The catalytic activity of our ligands was tested in the asymmetric hydrosilylation of styrene (Table 4).<sup>8,42</sup> Johannsen and co-workers have proposed two

Table 4. Pd-Catalyzed Hydrosilylation of Styrene

entry	ligand	L:Pd <sup>a</sup>	time (h)	conv <sup>b</sup> (%)	ee <sup>c</sup>
1	<b>2a</b>	1:1	6	>99	70% (R)
2	<b>2a</b>	2:1	24	>99	80% (R)
3	<b>2b</b>	1:1	48	65	17% (R)
4	<b>2b</b>	2:1	96	50	49% (R)
5	<b>3a</b>	1:1	48	11	17% (R)
6	<b>3a</b>	2:1	48	88	86% (R)
7	<b>3b</b>	1:1	48	15	73% (R)
8	<b>3b</b>	2:1	48	15	5% (S)
9	<b>4a</b>	1:1	6	86	28% (R)
10	<b>4a</b>	2:1	6	>99	20% (R)
11	<b>4b</b>	1:1	6	84	37% (R)
12	<b>4b</b>	2:1	6	>99	43% (R)
13	<b>5a</b>	1:1	16	>99	82% (R)
14	<b>5a</b>	2:1	16	>99	84% (R)
15	<b>5b</b>	1:1	16	>99	7% (R)
16	<b>5b</b>	2:1	16	>99	2% (R)

<sup>a</sup>Catalyst was generated *in situ* from ligand (0.25 mol% or 0.50 mol%) and  $[\text{Pd}(\text{allyl})\text{Cl}]_2$  (0.125 mol%) and reacted with styrene (10.0 mmol) and trichlorosilane (12.0 mmol). <sup>b</sup>Determined by  $^1\text{H}$  NMR spectroscopy. <sup>c</sup>Determined by chiral HPLC (Lux 5u Cellulose-1 column).

competitive cycles for this process.<sup>41</sup> According to their model, either one or two coordination sites can be occupied by phosphine ligands. In the case of a one-coordinate phosphine complex, the vacant site is filled with a  $\pi$ -coordinated substrate alkene or, alternatively, by utilizing the aromatic backbone of the MOP-type compound, which can act as a hemilabile binding site.<sup>42</sup> Conversely, when a ligand to palladium ratio of 2:1 is employed, the formation of an active catalytic species with two coordinated phosphorus ligands may be favored.<sup>41</sup>

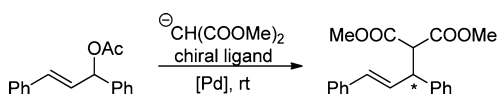
The catalysts were generated *in situ* by the reaction of the ligand with allylpalladium dimer. A ligand to palladium ratio of 1:1 or 2:1 was chosen to account for both possible catalytic pathways as described above and to selectively promote one pathway over the other. However, it should be noted that the complex formation is also dependent on the nature of the ligand, as we have seen from our coordination studies on palladium(II) (*vide supra*). The catalytic hydrosilylation reaction of styrene was carried out without additional solvent. Subsequent oxidation of the silane afforded 1-phenylethanol, the absolute configuration of which was determined. Notably, ligands **2a**, **4a,b**, and **5a,b** (entries 1, 2, 9–16) all showed complete consumption of the starting material in less than 24 h reaction time, whereas the OMe-substituted phosphirane **2b** (entries 3, 4) and dimethylphosphine derivatives **3a,b** (entries 5–8) are significantly less reactive in this transformation. Calculations on the reaction mechanism of the hydrosilylation suggest that the rate-determining step in the catalytic cycle is the reductive elimination.<sup>43</sup> Therefore, one might expect that the good donor ligands **3a,b** would be less active catalysts, as they favor the higher oxidation state on the metal. More surprising, then, were the high activity of the bis-(dimethylamino)phosphine ligands **4a,b**, which are also electron-rich, and the discrepancy in the performance of the phosphiranes **2a,b** (Table 4).

The best results were obtained with phosphirane **2a** and phosphonite **5a** (entries 1, 2 and 13, 14). Both show good activity and enantioselectivity of 70–84%. Their respective OMe-substituted derivatives **2b** and **5b** (entries 3, 4 and 15, 16) gave inferior selectivities in agreement with the reported values for OMe- and other 2'-substituted MOP ligands.<sup>44</sup> The bis(dimethylamino) derivatives **4a,b** (entries 9–12) gave low ee values (20–43%), despite being among the most catalytically active catalysts tested. The effect of the L:Pd ratio on the reaction was found to be limited, and only in the case of **3a,b** (entries 5–8) did we find more pronounced deviations. The inconsistencies may be caused by the overall low activity for **3a,b** as no complete substrate conversions were achieved, but notably in our coordination studies, the dimethylphosphine ligand **3b** was the only derivative that gave the palladium complex **19b** with a L:Pd ratio of 2:1 (*vide supra*). Ligands **2a,b**, **4a,b**, and **5a,b** appear to favor the formation of complexes in a 1:1 ratio of L:Pd, even when an excess of ligand is used.

**Asymmetric Allylic Alkylation.** As another common benchmark reaction, we investigated the asymmetric allylic alkylation of (*rac*)-(E)-1,3-diphenylallyl acetate (Table 5).<sup>45</sup> The nucleophile was generated from dimethyl malonate and bis(trimethylsilyl)acetamide (BSA). This reaction follows a different mechanism than the hydrosilylation one and hence is expected to show an alternative outcome for the investigated ligands. The oxidative addition is regarded as possibly rate-determining, and thus a good donor ligand would be necessary. The subsequent nucleophilic substitution furnishes an energetic barrier that favors electron-withdrawing ligands, but in contrast to the oxidative addition the reaction step is irreversible.<sup>46</sup>

The activity of the catalysts correlates with the net donor strength of the ligands (Table 1 and 5). Consequently, the fastest catalysts were found in **3a,b** ligated complexes, giving conversions within less than 4 h (Table 5, entries 3, 4). Good catalytic activities were also found for **4a,b** (entries 5–8) but to a lesser extent for **2a,b** (entries 1, 2). Reactions with the phosphonite ligands **5a,b** were incomplete, even after prolonged reaction times (entries 9, 10), most likely as a result



**Table 5. Palladium-Catalyzed Asymmetric Allylic Alkylation of (*rac*)-(E)-1,3-Diphenylallyl Acetate**


entry	ligand <sup>a</sup>	L: Pd	time <sup>b</sup> (h)	yield <sup>c</sup> (%)	ee <sup>d</sup>
1	2a	2:1	22	91	17% ( <i>r</i> )
2	2b	2:1	22	93	1% ( <i>s</i> )
3	3a	2:1	3	91	41% ( <i>r</i> )
4	3b	2:1	4	98	14% ( <i>r</i> )
5	4a	2:1	5	89	66% ( <i>s</i> )
6	4a	1:1	6	86	67% ( <i>s</i> )
7	4b	2:1	5	88	13% ( <i>s</i> )
8	4b	1:1	6	95	12% ( <i>s</i> )
9	5a	2:1	48	20	15% ( <i>r</i> )
10	5b	2:1	48	2	29% ( <i>r</i> )

<sup>a</sup>Catalyst was generated *in situ* from ligand (8.0 mol% or 4.0 mol%) and [Pd(allyl)Cl]<sub>2</sub> (2.0 mol%) and reacted with (*rac*)-(E)-1,3-diphenylallyl acetate (0.5 mmol), dimethyl malonate (1.0 mmol), BSA (1.0 mmol), and KOAc (0.05 mmol). <sup>b</sup>Reaction progress was monitored by TLC analysis until full conversion was observed (except for entries 9, 10). <sup>c</sup>Isolated yield after column chromatographic workup. <sup>d</sup>Determined by chiral HPLC (Daicel Chiralpak AD-H Column).

of their poor  $\sigma$ -donor character. The best enantioselectivities were achieved with ligands **3a** (41% ee (*R*)) and **4a** (66–67% ee (*S*)), interestingly yielding their major enantiomers in opposite absolute configurations. In the case of **4a,b** we checked for the influence of the L: Pd ratio (2:1 versus 1:1, entries 5–8), but the reaction gave virtually the same outcome.

## CONCLUSIONS

Primary phosphines are versatile ligand precursors that can give rise to a variety of phosphorus compounds. Here, we report preparations of ligands **2a,b**, **4a,b**, and **5a,b** as well as a simplified synthesis of **3a,b**, which were achieved in straightforward two-step, one-pot reaction approaches.

We have discussed the unique electronic and steric properties of these different P-ligand functionalities, how they compare with each other, and how this is manifested in their platinum(II) and palladium(II) metal complexes. The highly strained phosphiranes **2a,b** have exceptional thermal stability and show remarkably low *trans* influence, but equally enhanced *cis* influence, in their platinum(II) complexes as a result of the high *s*-character of their donor orbital. Their poor donor but good acceptor characteristics compare best to the phosphonites **5a,b**. These ligands are best employed in catalytic reactions such as hydrosilylations, where the reductive elimination step has been proposed to be rate-determining.<sup>43</sup> Interestingly, the small size of the P-substituents in **2a,b** adding to the MOP backbone seems to have little detrimental effect on the enantioselectivities; the steric burden of the phosphirane unit is minimal, yet ee's of up to 80% were obtained using **2a**. Similarly, good results were obtained with the phosphonite **5a**, yielding up to 84% ee.

Different electronic characteristics are evident in the electron-rich  $\sigma$ -donor ligands, the dimethylphosphines **3a,b** and the bis(dimethylamino)phosphines **4a,b**. The donor properties of **4a,b** seem adaptable to some extent by transferring electron density from either one or two of their nitrogen lone pairs onto the phosphorus (indicated by the

degree of distortion around the nitrogen atom). It may be for this reason that, although usually being good donor ligands, **4a,b** still show high activity in the hydrosilylation reaction. They are also effective in the allylic alkylation reaction, for which we observed enantioselectivities of up to 67%. Notably, the absolute configuration of the major product was reversed when **4a,b** were used compared to the dimethylphosphines **3a,b**. That MOP-type phosphines can act as hemilabile ligands via coordination of their aryl backbone has been unambiguously shown by crystallographic analysis of **18b**. However, hemilabile binding to saturate the coordination sphere of the metal center may be disfavored when a second P-donor ligand is available. The prominent active species in both catalytic transformations is still somewhat speculative, and further investigations are underway.

## ASSOCIATED CONTENT

### Supporting Information

Full experimental procedures and crystallographic data. This material is available free of charge via the Internet at <http://pubs.acs.org>.

## AUTHOR INFORMATION

### Corresponding Author

\* E-mail: [lee.higham@ncl.ac.uk](mailto:lee.higham@ncl.ac.uk). Fax: (+44) 191 222 6929. Tel: (+44) 191 222 5542.

### Notes

The authors declare no competing financial interest.

## ACKNOWLEDGMENTS

We thank the EPSRC for a Career Acceleration Fellowship (L.J.H.), a Studentship (A.F.), its National Mass Spectrometry Service Centre, Swansea, UK, and a crystallography Equipment Grant. We thank Prof. William McFarlane (Newcastle University) for valuable NMR advice and experiments, and Johnson Matthey for the loan of platinum metal salts.

## REFERENCES

- (1) Noyori, R. *Angew. Chem., Int. Ed.* **2002**, *41*, 2008–2022.
- (2) Tolman, C. A. *Chem. Rev.* **1977**, *77*, 313–348.
- (3) See, for example: (a) Kühl, O. *Coord. Chem. Rev.* **2005**, *249*, 693–704. (b) Brown, T. L.; Lee, K. J. *Coord. Chem. Rev.* **1993**, *128*, 89–116. (c) Flanagan, S. P.; Guiry, P. J. *J. Organomet. Chem.* **2006**, *691*, 2125–2154. (d) Fey, N.; Orpen, A. G.; Harvey, J. N. *Coord. Chem. Rev.* **2009**, *253*, 704–722. (e) Jover, J.; Fey, N.; Harvey, J. N.; Lloyd-Jones, G. C.; Orpen, A. G.; Owen-Smith, G. J. J.; Murray, P.; Hose, D. R. J.; Osborne, R.; Purdie, M. *Organometallics* **2010**, *29*, 6245–6258. (f) Jover, J.; Fey, N.; Harvey, J. N.; Lloyd-Jones, G. C.; Orpen, A. G.; Owen-Smith, G. J. J.; Murray, P.; Hose, D. R. J.; Osborne, R.; Purdie, M. *Organometallics* **2012**, *31*, 5302–5306. (g) Fey, N.; Garland, M.; Hopewell, J. P.; McMullin, C. L.; Mastroianni, S.; Orpen, A. G.; Pringle, P. G. *Angew. Chem., Int. Ed.* **2012**, *51*, 118–122. (h) Cooney, K. D.; Cundari, T. R.; Hoffmann, N. W.; Pittard, K. A.; Danielle Temple, M.; Zhao, Y. *J. Am. Chem. Soc.* **2003**, *125*, 4318–4324.
- (4) (a) Hiney, R. M.; Higham, L. J.; Müller-Bunz, H.; Gilheany, D. G. *Angew. Chem., Int. Ed.* **2006**, *45*, 7248–7251. (b) Ficks, A.; Sibbald, C.; Ojo, S.; Harrington, R. W.; Clegg, W.; Higham, L. J. *Synthesis* **2013**, *45*, 265–271. (c) Stewart, B.; Harriman, A.; Higham, L. J. *Organometallics* **2011**, *30*, 5338–5343.
- (5) (a) Han, J. W.; Hayashi, T. *Tetrahedron: Asymmetry* **2010**, *21*, 2193–2197. (b) Hayashi, T. *Acc. Chem. Res.* **2000**, *33*, 354–362.
- (6) Lagasse, F.; Kagan, H. B. *Chem. Pharm. Bull.* **2000**, *48*, 315–324.
- (7) Kočovský, P.; Vyskočil, S.; Smrčina, M. *Chem. Rev.* **2003**, *103*, 3213–3245 and references therein.

- (8) (a) Hayashi, T.; Hirate, S.; Kitayama, K.; Tsuji, H.; Torii, A.; Uozumi, Y. *J. Org. Chem.* **2001**, *66*, 1441–1449. (b) Hayashi, T. *Acta Chem. Scand.* **1996**, *50*, 259–266.
- (9) (a) Clarke, E. F.; Rafter, E.; Müller-Bunz, H.; Higham, L. J.; Gilheany, D. G. *J. Organomet. Chem.* **2011**, *696*, 3608–3615. (b) Armanino, N.; Koller, R.; Togni, A. *Organometallics* **2010**, *29*, 1771–1777. (c) Saha, B.; RajanBabu, T. V. *J. Org. Chem.* **2007**, *72*, 2357–2363. (d) Xie, X.; Zhang, T. Y.; Zhang, Z. *J. Org. Chem.* **2006**, *71*, 6522–6529. (e) Hamada, T.; Chieffi, A.; Åhman, J.; Buchwald, S. L. *J. Am. Chem. Soc.* **2002**, *124*, 1261–1268. (f) Chen, J.-X.; Daeuble, J. F.; Stryker, J. M. *Tetrahedron* **2000**, *56*, 2789–2798.
- (10) (a) Maier, L. In *Organic Phosphorus Compounds*, Vol. 1; Kosolapoff, G. M., Maier, L., Eds.; Wiley-Interscience: New York, 1972; pp 4–16. (b) Higham, L. J. In *Phosphorus Compounds: Advanced Tools in Catalysis and Material Sciences, Catalysis by Metal Complexes*, Vol. 37; Peruzzini, M., Gonsalvi, L., Eds.; Springer: Berlin, Germany, 2011; pp 1–19.
- (11) (a) Ficks, A.; Martinez-Botella, I.; Stewart, B.; Harrington, R. W.; Clegg, W.; Higham, L. J. *Chem. Commun.* **2011**, *47*, 8274–8276. (b) Mézailles, N.; Fanwick, P. E.; Kubiak, C. P. *Organometallics* **1997**, *16*, 1526–1530.
- (12) (a) Mathey, F. *Chem. Rev.* **1990**, *90*, 997–1025. (b) Quin, L. D. *A Guide to Organophosphorus Chemistry*; John Wiley and Sons: New York, 2000; pp 234–241. (c) Mathey, F.; Regitz, M. In *Phosphorus-Carbon Heterocyclic Chemistry: The Rise of a New Domain*; Mathey, F., Ed.; Elsevier Science: Amsterdam, 2001; pp 17–55.
- (13) (a) Shi, M.; Chen, L.-H.; Li, C.-Q. *J. Am. Chem. Soc.* **2005**, *127*, 3790–3800. (b) Shi, M.; Li, C.-Q. *Tetrahedron: Asymmetry* **2005**, *16*, 1385–1391. (c) Shi, M.; Liu, X.-G.; Guo, Y.-W.; Zhang, W. *Tetrahedron* **2007**, *63*, 12731–12734.
- (14) Weferling, N. Z. *Anorg. Allg. Chem.* **1987**, *548*, 55–62.
- (15) (a) Orthaber, A.; Fuchs, M.; Belaj, F.; Rechberger, G. N.; Kappe, C. O.; Pietschnig, R. *Eur. J. Inorg. Chem.* **2011**, 2588–2596. (b) Starosta, R.; Bykowska, A.; Barys, M.; Wieliczko, A. K.; Staroniewicz, Z.; Jeżowska-Bojczuk, M. *Polyhedron* **2011**, *30*, 2914–2921. (c) Clarke, M.; Cole-Hamilton, D. J.; Slawin, A. M. Z.; Woollins, J. D. *Chem. Commun.* **2000**, 2065–2066. (d) Clarke, M. L.; Holliday, G. L.; Slawin, A. M. Z.; Woollins, J. D. *J. Chem. Soc., Dalton Trans.* **2002**, 1093–1103. (e) Dyer, P. W.; Fawcett, J.; Hanton, M. J.; Kemmitt, R. D. W.; Padda, R. *Dalton Trans.* **2003**, 104–113. (f) Cheng, J.; Wang, F.; Xu, J.-H.; Pan, Y.; Zhang, Z. *Tetrahedron Lett.* **2003**, *44*, 7095–7098.
- (16) Gopalakrishnan, J. *Appl. Organomet. Chem.* **2009**, *23*, 291–318.
- (17) (a) McFarlane, W.; Rycroft, D. S. *J. Chem. Soc., Dalton Trans.* **1973**, 2162–2166. (b) McFarlane, W.; Rycroft, D. S. *J. Chem. Soc., Chem. Commun.* **1972**, 902–903.
- (18) (a) Allen, D. W.; Taylor, B. F. *J. Chem. Soc., Dalton Trans.* **1982**, 51–54. (b) Pinnell, R. P.; Megerle, C. A.; Manatt, S. L.; Kroon, P. A. *J. Am. Chem. Soc.* **1973**, *95*, 977–978.
- (19) Muller, A.; Otto, S.; Roodt, A. *Dalton Trans.* **2008**, 650–657.
- (20) (a) Roodt, A.; Otto, S.; Steyl, G. *Coord. Chem. Rev.* **2003**, *245*, 121–137. (b) Otto, S.; Roodt, A. *Inorg. Chim. Acta* **2004**, *357*, 1–10.
- (21) Kemp, G.; Roodt, A.; Purcell, W. *Rhodium Expr.* **1995**, *12*, 21–26.
- (22) (a) Liedtke, J.; Loss, S.; Alcaraz, G.; Gramlich, V.; Grützmacher, H. *Angew. Chem., Int. Ed.* **1999**, *38*, 1623–1626. (b) Liedtke, J.; Loss, S.; Widauer, C.; Grützmacher, H. *Tetrahedron* **2000**, *56*, 143–156. (c) Liedtke, J.; Rüegger, H.; Loss, S.; Grützmacher, H. *Angew. Chem., Int. Ed.* **2000**, *39*, 2478–2481. (d) Laporte, C.; Frison, G.; Grützmacher, H.; Hillier, A. C.; Sommer, W.; Nolan, S. P. *Organometallics* **2003**, *22*, 2202–2208.
- (23) (a) Senn, H. M.; Deubel, D. V.; Blöchl, P. E.; Togni, A.; Frenking, G. *J. Mol. Struct., Thechem.* **2000**, *506*, 233–242. (b) Fey, N.; Tsipis, A. C.; Harris, S. E.; Harvey, J. N.; Orpen, A. G.; Mansson, R. A. *Chem.—Eur. J.* **2006**, *12*, 291–302.
- (24) Carreira, M.; Charensuk, M.; Eberhard, M.; Fey, N.; van Ginkel, R.; Hamilton, A.; Mul, W. P.; Orpen, A. G.; Phetmung, H.; Pringle, P. G. *J. Am. Chem. Soc.* **2009**, *131*, 3078–3092.
- (25) Dunne, B. J.; Morris, R. B.; Orpen, A. G. *J. Chem. Soc., Dalton Trans.* **1991**, 653–661.
- (26) Müller, T. E.; Mingos, D. M. P. *Transition Met. Chem.* **1995**, *20*, 533–539.
- (27) For an overview of steric and electronic descriptors, see: Fey, N. *Dalton Trans.* **2010**, 39, 296–310.
- (28) Mathew, J.; Thomas, T.; Suresh, C. H. *Inorg. Chem.* **2007**, *46*, 10800–10809.
- (29) For reviews on  $^{195}\text{Pt}$  NMR, see: (a) Still, B. M.; Kumar, P. G. A.; Aldrich-Wright, J. R.; Price, W. S. *Chem. Soc. Rev.* **2007**, *36*, 665–686. (b) Pregosin, P. S. *Coord. Chem. Rev.* **1982**, *44*, 247–291. (c) Pregosin, P. S. *Annu. Rep. NMR Spectrosc.* **1986**, *17*, 285–349. (d) Kennedy, J. D.; McFarlane, W.; Puddephatt, R. J.; Thompson, P. J. *J. Chem. Soc., Dalton Trans.* **1976**, 874–879.
- (30) Mather, G. G.; Pidcock, A.; Rapsey, G. J. N. *J. Chem. Soc., Dalton Trans.* **1972**, 19, 2095–2099.
- (31) (a) Waddell, P. G.; Slawin, A. M. Z.; Woollins, J. D. *Dalton Trans.* **2010**, 39, 8620–8625. (b) Cobley, C. J.; Pringle, P. G. *Inorg. Chim. Acta* **1997**, *265*, 107–115.
- (32) Appleton, T. G.; Clark, H. C.; Manzer, L. E. *Coord. Chem. Rev.* **1973**, *10*, 335–422.
- (33) (a) Rigamonti, L.; Manassero, C.; Rusconi, M.; Manassero, M.; Pasini, A. *Dalton Trans.* **2009**, 1206–1213. (b) Münzenberg, R.; Rademacher, P.; Boese, R. *J. Mol. Struct.* **1998**, *444*, 77–90.
- (34) Anderson, K. M.; Orpen, A. G. *Chem. Commun.* **2001**, 2682–2683.
- (35) (a) Clendenning, S. B.; Hitchcock, P. B.; Lawless, G. A.; Nixon, J. F.; Tate, C. W. *J. Organomet. Chem.* **2010**, *695*, 717–720. (b) Atherton, M. J.; Fawcett, J.; Hill, A. P.; Holloway, J. H.; Hope, E. G.; Russell, D. R.; Saunders, G. C.; Stead, R. M. *J. Chem. Soc., Dalton Trans.* **1997**, 1137–1147.
- (36) See for example: (a) Breutel, C.; Pregosin, P. S.; Salzmänn, R.; Togni, A. *J. Am. Chem. Soc.* **1994**, *116*, 4067–4068. (b) Scheele, U. J.; John, M.; Dechert, S.; Meyer, F. *Eur. J. Inorg. Chem.* **2008**, 373–377. (c) Ketz, B. E.; Cole, A. P.; Waymouth, R. M. *Organometallics* **2004**, *23*, 2835–2837. (d) Peng, H. M.; Song, G.; Li, Y.; Li, X. *Inorg. Chem.* **2008**, *47*, 8031–8043. (e) Filipuzzi, S.; Pregosin, P. S.; Calhorda, M. J.; Costa, P. J. *Organometallics* **2008**, *27*, 2949–2958. (f) Ficks, A.; Hiney, R. M.; Harrington, R. W.; Gilheany, D. G.; Higham, L. J. *Dalton Trans.* **2012**, *41*, 3515–3522.
- (37) (a) Hayashi, T.; Iwamura, H.; Naito, M.; Matsumoto, Y.; Uozumi, Y.; Miki, M.; Yanagi, K. *J. Am. Chem. Soc.* **1994**, *116*, 775–776. (b) Kumar, P. G. A.; Dotta, P.; Hermatschweiler, R.; Pregosin, P. S.; Albinati, A.; Rizzato, S. *Organometallics* **2005**, *24*, 1306–1314.
- (38) (a) Kočovský, P.; Vyskočil, Š.; Čisarová, I.; Sejbál, J.; Tišlerová, I.; Smrčina, M.; Lloyd-Jones, G. C.; Stephen, S. C.; Butts, C. P.; Murray, M.; Langer, V. *J. Am. Chem. Soc.* **1999**, *121*, 7714–7715. (b) Dotta, P.; Kumar, P. G. A.; Pregosin, P. S.; Albinati, A.; Rizzato, S. *Organometallics* **2004**, *23*, 4247–4254. (c) Dotta, P.; Kumar, P. G. A.; Pregosin, P. S.; Albinati, A.; Rizzato, S. *Helv. Chim. Acta* **2004**, *87*, 272–278. (d) Dotta, P.; Kumar, P. G. A.; Pregosin, P. S.; Albinati, A.; Rizzato, S. *Organometallics* **2003**, *22*, 5345–5349. (e) Mikhel, I. S.; Rüegger, H.; Butti, P.; Camponovo, F.; Huber, D.; Mezzetti, A. *Organometallics* **2008**, *27*, 2937–2948.
- (39) (a) Pregosin, P. S. *Chem. Commun.* **2008**, 4875–4884. (b) Pregosin, P. S. *Coord. Chem. Rev.* **2008**, *252*, 2156–2170.
- (40) See, for example: (a) Lloyd-Jones, G. C.; Stephen, S. C.; Murray, M.; Butts, C. P.; Vyskočil, Š.; Kočovský, P. *Chem.—Eur. J.* **2000**, *6*, 4348–4357. (b) Kawatsura, M.; Uozumi, Y.; Ogasawara, M.; Hayashi, T. *Tetrahedron* **2000**, *56*, 2247–2257. (c) Camus, J.-M.; Andrieu, J.; Richard, P.; Poli, R. *Eur. J. Inorg. Chem.* **2004**, 1081–1091. (d) Ficks, A.; Sibbald, C.; John, M.; Dechert, S.; Meyer, F. *Organometallics* **2010**, *29*, 1117–1126.
- (41) Pedersen, H. L.; Johannsen, M. *J. Org. Chem.* **2002**, *67*, 7982–7994.
- (42) Gibson, S. E.; Rudd, M. *Adv. Synth. Catal.* **2007**, *349*, 781–795.
- (43) (a) Magistrato, A.; Togni, A.; Rothlisberger, U. *Organometallics* **2006**, *25*, 1151–1157. (b) Magistrato, A.; Woo, T. K.; Togni, A.; Rothlisberger, U. *Organometallics* **2004**, *23*, 3218–3227.

- (44) Kitayama, K.; Uozumi, Y.; Hayashi, T. *J. Chem. Soc., Chem. Commun.* **1995**, 1533–1534.
- (45) Lu, Z.; Ma, S. *Angew. Chem., Int. Ed.* **2008**, *47*, 258–297 and references therein.
- (46) Poli, G.; Prestat, G.; Liron, F.; Kammerer-Pentier, C. *Top. Organomet. Chem.* **2012**, *38*, 1–64.